Protoplasma (2019) 256:131–146
https://doi.org/10.1007/s00709-018-1284-3

ORIGINAL ARTICLE

# Cytological differentiation and cell wall involvement in the growth mechanisms of articulated laticifers in *Tabernaemontana catharinensis* A.DC. (Apocynaceae)

Yve Canaveze[1] · Alexandra Antunes Mastroberti[2] · Jorge Ernesto de Araujo Mariath[2] · Silvia Rodrigues Machado[1]

Received: 28 March 2018 / Accepted: 3 July 2018 / Published online: 11 July 2018


## Abstract

The cellular mechanisms of laticifer growth are of particular interest in plant biology but are commonly neglected. Using transmission electron microscopy and immunocytochemical methods, we recorded cytological differentiation and evaluated the cell wall involvement in the growth of articulated laticifers with intrusive growth in the mature embryo and plant shoot apex of *Tabernaemontana catharinensis*. The incorporation of adjacent meristematic cells into the laticifer system occurred in the embryo and plant shoot apex, and the incorporated cells acquired features of laticifer, confirming the laticifers' action-inducing mechanism. In the embryo, this was the main growth mechanism, and began with enlargement of the plasmodesmata and the formation of pores between laticifers and meristematic cells. In the plant shoot apex, it began with loose and disassembled walls and the reorientation of the cortical microtubules of the incorporated cell. Plasmodesmata were absent in these laticifers. There was stronger evidence of intrusive growth in undifferentiated portions of the plant shoot apex than in the embryo. The numerous plasmodesmata in laticifers of the embryo may have been related to the lower frequency of intrusive growth. Intrusive growth was associated with presence of arabinan (increasing wall flexibility and fluidity), and absence of galactan (avoiding wall stiffness), and callose (as a consequence of reduction in symplastic connections) in the laticifer walls. The abundance of low de-methyl-esterified homogalacturonan in the middle lamella and corners may reestablish cell-cell bonding in the laticifers. The cell wall features differed between embryo and plant shoot apex and are directly associated to laticifer growth mechanisms.

**Keywords** Immunocytochemistry · Intrusive growth · Laticifer system · Laticifers' action-inducing mechanism · Ultrastructure

## Introduction

Laticifers are single cells or a series of connected cells that synthesize and accumulate latex and form a system that permeates different tissues of the plant body (Evert 2006). Laticifers are grouped into articulated and nonarticulated types based on their ontogenesis and structure, and both types vary in their degree of structural complexity (Esau 1965; Fahn 1979; Evert 2006). Despite the widespread presence of laticifers in angiosperms, ca. 10% of all flowering plants, little information is available regarding the mechanisms of laticifer cell differentiation (Castelblanque et al. 2016). Detailed cytological analysis of laticifers from a developmental point of view, particularly regarding the mechanisms of laticifer growth, are of particular interest in plant biology.

A previous anatomical study of *Tabernaemontana catharinensis*, an Apocynaceae species, revealed that this species has articulated anastomosing laticifers with a complex structure, and a developmental mechanism involving protoplast fusion, the addition of adjacent cells, and intrusive growth, which occur in mature embryos, seedlings, and plants (Canaveze and Machado 2016). Intrusive growth is commonly associated with nonarticulated

Handling Editor: Alexander Schulz

✉ Yve Canaveze
yve.canaveze@yahoo.com.br

[1] Department of Botany, Institute of Biosciences, Universidade Estadual Paulista – UNESP, Botucatu, São Paulo, Brazil

[2] Laboratory of Plant Anatomy, Department of Botany, Universidade Federal do Rio Grande do Sul, Porto Alegre, Brazil

laticifers (Mahlberg 1993), while protoplast fusion and the addition of adjacent cells have been linked to articulated laticifers (Milanez 1959, 1977; Lopes et al. 2009). Remarkably, our study (Canaveze and Machado 2016) showed that such growth mechanisms occur simultaneously during the development of articulated laticifers in the same species and have been observed in distinct vegetative developmental stages. Cellular changes associated with the mechanism that drives the incorporation of cells into the laticifer system have been described in mature embryos (Milanez 1959, 1977), but no ultrastructural studies of the laticifers' action-inducing mechanism in other vegetative developmental stages have been conducted.

Intrusive growth involves preexisting parts of the cell remaining in their original locations while new parts change their positions in relation to other cells and occupy new locations (Lev-Yadun 2001). This growth mechanism is a neglected feature of plant-cell interactions. Cell wall changes linked to intrusive growth include the disassembly or rearrangement of cell wall compounds and the breaking of plasmodesmatal connections among laticifers and adjacent cells (Mahlberg 1993; Serpe et al. 2002). Immunocytochemical methods have shown potential in elucidating cell wall dynamics during the development of laticifers, particularly intrusive growth (Serpe et al. 2001, 2002, 2004). The cell walls of laticifers and adjacent meristematic cells differ in the expression of (1→4)-β-galactan epitope and callose, being less abundant or absent in laticifers in the Apocynaceae (Serpe et al. 2002) and Euphorbiaceae (Serpe et al. 2004). Such features are associated with intrusive growth in nonarticulated laticifers. In addition, large amounts of (1→5)-α-arabinan epitope in laticifer walls and the middle lamella between laticifers and adjacent cells rich in homogalacturonan (HG) with a low degree of methyl esterification also appear to be related to intrusive growth (Serpe et al. 2001, 2002). However, these latter features seem to reflect species-specific patterns of epitope occurrence (Serpe et al. 2004). It is remarkable that these studies were performed on nonarticulated laticifers present in the plant shoot apex. To the best of our knowledge, there is no information available regarding polysaccharide changes in articulated laticifers. Based on polysaccharides changing in nonarticulated laticifers during intrusive growth (Serpe et al. 2001, 2002, 2004), we hypothesized that glycan distributions in the cell walls of articulated laticifers, in both the mature embryo and the plant shoot apex, might support the same intrusive process as in nonarticulated laticifers.

The aim of the study was to analyze the cytology and cell wall polysaccharide distribution of articulated laticifers in *T. catharinensis* from a developmental perspective, and investigate whether these differ in mature embryos and plant shoot apices. In particular, we explored protoplast and cell wall changes in laticifers and adjacent cells by investigating protoplast fusion, laticifers driving the incorporation of adjacent cells, and the intrusive growth mechanism using transmission electron microscopy (TEM) and immunocytochemical methods.

## Material and methods

### Plant material

We studied mature embryos and plant shoot apices of *T. catharinensis*. To obtain these specimens, we collected seeds from mature fruits of *T. catharinensis* plants growing in areas of cerrado (savanna-like vegetation) localized in the municipalities of Botucatu (22° 42′ 21.4″ S and 48° 18′ 23.7″ W; 22° 51′ 16.8″ S and 48° 25′ 53.2″ W) and Pratânia (22° 48′ 48.8″ S and 48° 44′ 33.7″ W) in São Paulo state, Brazil, during 2010, 2011, 2013, and 2014 (BOTU Herbarium, Voucher Nos. 27625–27627). We removed mature embryos from soaked seeds and cultivated 80-day-old plants under light- and temperature-controlled conditions (Canaveze and Machado 2015).

We collected and processed samples from the cotyledonary nodal region of mature embryos with nondifferentiated plumules (Canaveze and Machado 2015) and from the third phytomer to the shoot apex of 80-day-old plants.

### Methods for TEM

We fixed the samples for 24 h at 5 °C in 2.5% glutaraldehyde in 0.1 M phosphate buffer (pH 7.3) and then post-fixed them in a 1% osmium tetroxide ($OsO_4$) aqueous solution for 2 h at 25 °C in the same buffer. We dehydrated the samples in an acetone series and embedded them in Araldite resin (Araldite 502, Electron Microscopy Sciences, Hatfield, USA). The ultrathin sections were stained with a saturated aqueous solution of uranyl acetate followed by lead citrate (Reynolds 1963) and then examined them with a transmission electron microscope (Tecnai Spirit, FEI Company, Germany) at 80 kV.

### Immunocytochemistry

#### Fixation, dehydration, embedding, and sectioning

We fixed the samples for 48 h in 1% [*v*/*v*] glutaraldehyde and 4% [*w*/*v*] commercial formaldehyde in 0.1 M phosphate buffer (pH 7.2) (McDowel and Trump 1976). Samples to analyze in TEM were post-fixed in a 1% [*v*/*v*] osmium tetroxide ($OsO_4$) aqueous solution for 1 h at 25 °C in the same buffer.

For experiments involving localization of callose, we incubated some samples with the inhibitor of callose synthesis 2-deoxy-D-glucose (DDG) at $10^{-4}$ M for 1 h at 25 °C prior to fixation (Gale et al. 1984; Radford et al. 1998; Serpe et al. 2002) to avoid the callose epitope being deposited by injury. Subsequently, samples were fixed as described previously.

We dehydrated all samples in an alcohol series, embedded them in LR White resin (Hard Grade - London Resin Company) and polymerized them in gelatin capsules at 50 °C for 24 h. Semi-thin (500 nm) sections of samples were made with glass knives in a microtome (Leica RM 2165) and collected on glass slides coated with poly-L-lysine (Sigma-Aldrich). Sections were stained with toluidine blue pH 4.7 (O'Brien et al. 1964), mounted in water and observed under bright-field microscopy. Ultrathin sections (80 nm) of samples post-fixed in $OsO_4$ with a Diatome diamond knife were made and collected in 200 mesh gold grids.

### Immunofluorescence microscopy

Antibody selection was based on differential labeling between nonarticulated laticifers and adjacent cells in studies using a range of monoclonal antibodies (MAbs) against HG, rhamnogalacturonan I, arabinogalactan proteins, and β-D-glucans, and a polyclonal antibody against xyloglucan in the shoot apices of *Asclepias speciosa* (Apocynaceae, Serpe et al. 2001, 2002) and *Euphorbia heterophylla* (Euphorbiaceae, Serpe et al. 2004).

We used three MAbs directed against pectin epitopes, such as JIM5, LM5, and LM6 (Plant Probes, Leeds, UK) (Table 1). JIM5 recognize HG epitopes with high degrees of methyl esterification (Willats et al. 2000). LM5 and LM6 recognize (1→4)-β-D-galactans (Jones et al. 1997) and (1→5)-α-L-arabinans, respectively (Willats et al. 1998). The sections were hydrated with phosphate-buffered saline (PBS) at pH 7.1 (Harris 1994) and blocked to prevent nonspecific binding with a 3% milk protein solution in PBS (MP/PBS). In sequence, the sections were incubated in a 1:10 dilution of primary antibody in MP/PBS for 2 h. After washing with PBS, slides were incubated in a 1:100 dilution of anti-rat-IgG (whole molecule) linked to fluorescein isothiocyanate (FITC, Sigma-Aldrich) in MP/PBS for 2 h. We also used a MAb to detect callose ((1→3)-β-D-glucans; BS400-2) (Meikle et al. 1991) (Biosupplies Australia, Parkville, Australia) (Table 1). Sections were hydrated and blocked before incubation in a 1:200 dilution of BS400-2 in MP/PBS for 2 h. After washing, these sections were incubated in a 1:100 dilution of goat anti-mouse-IgG (whole molecule) linked to FITC (Sigma-Aldrich) in MP/PBS for 1 h. Slides were mounted in 0.1% [*w*/*v*] paraphenylenediamine (PPD) in glycerol.

Furthermore, pretreatment for pectic HG removal with a first step in $Na_2CO_3$ 0.1 M and a second step in enzymatic solution of pH 11.4/pectate lyase (from *Aspergillus* sp., Megazyme) in Tris-HCl buffer, pH 8.0, was performed prior to labeling with LM5 and LM6 because pectic HG may mask sets of hemicellulose and other pectin epitopes (Marcus et al. 2008; Hervé et al. 2009, 2011).

After incubation with secondary antibody, we washed the sections with PBS and incubated them with 0.01% Calcofluor white (Fluorescent Brightener 28, Sigma-Aldrich) for 5 min. Slides were mounted with an anti-fade solution consisting of 0.1% PPD (Sigma-Aldrich) in 1:9 10 mM sodium phosphate buffer: 0.15 M NaCl and 90% glycerol. All steps were performed at room temperature (~25 °C).

Observations were made with a microscope equipped with epifluorescence (excitation filter 450–490 nm; microscope Leica DMR). Controls were made by omitting incubation with the primary antibody and did not show labeling by fluorochrome FITC (data not shown). Some sections embedded in LR White resin of mature embryo and plant shoot apex, which were not subjected to any either treatment or incubation, were checked and did not exhibit autofluorescence (data not shown).

Serial sections of the shoot apex of plants ($n = 3$) and cotyledonary node of mature embryos ($n = 3$) were used for all treatments. We compared samples of the shoot apex ($n = 3$) and cotyledonary node ($n = 3$) previously fixed with DDG with samples not previously fixed to control BS400-2 antibody.

### Immunogold labeling for TEM

To properly analyze the glycan distribution throughout the cell walls, ultrathin sections (70 nm) on gold grids were hydrated in PBS and blocked in MP/PBS. These sections were incubated with the MAbs as mentioned in the "Immunofluorescence microscopy" section. After rinsing with PBS, sections were incubated with the appropriate secondary antibodies conjugated to 10-nm colloidal gold. Binding of JIM5, LM5, and LM6 to the sections was detected using goat anti-rat IgG (*whole molecule*)-Gold (Sigma-Aldrich). Prior to labeling with LM5 and LM6, we performed incubation of some sections with pectate lyase (as described in "Immunofluorescence microscopy"). BS400-2 was detected using goat anti-mouse IgG (*whole molecule*)-Gold (Sigma-Aldrich). To avoid the callose epitope being deposited by injury, sections labeled with BS400-2 were prefixed with DDG.

We applied secondary antibodies at a 1:20 dilution in MP/PBS for 2 h. Subsequently, the sections were washed in PBS and then in distilled water. The incubations with primary antibody and both antibodies were suppressed in some sections and did not exhibit labeling (data not shown). All steps were performed at room temperature (~25 °C). We examined the material with a transmission electron microscope (FEI Tecnai™) at 80 kV.

The density of labeling (the number of gold particles per $\mu m^2$) in cell walls of laticifers and adjacent cells in mature embryo and plant shoot apex (in undifferentiated and differentiated portions) were determined by morphometric analysis using ImageJ software (Schindelin et al. 2012). Values were reported as the mean ± standard deviation of measurements ($n = 3$) made in electron micrographs.

**Table 1** Binding of the monoclonal antibodies to laticifer walls in mature embryo and plant shoot apex, comparing with adjacent cell walls, in *Tabernaemontana catharinensis* A.DC. The number of signals indicates the intensity of the reaction (+) weak, (++) moderate and (+++) intense; or (−) no labeling. LM = Leeds Monoclonal, JIM = John Innes Monoclonal, BS = Biosupplies Australia

| Monoclonal Antibodies | Epitopes | Mature embryo—cell walls | | Shoot apex of plants—cell walls | | | |
|---|---|---|---|---|---|---|---|
| | | Laticifers | Ground meristem cells | Laticifers in undifferentiated portion | Meristematic cells | Laticifers in differentiated portion | Parenchyma cells |
| JIM5 | HGs with low degree of methyl esterification | + | + | +++ (corners) | + | + (junction zones) | + (junction zones) |
| LM5 | (1→4)-β-D-galactans | – | – | – | + | ++ | ++ |
| LM6 | (1→5)-α-L-arabinans | + | + | +++ | + | – | – |
| BS400-2 | Callose | + | + | – | – | – | + |

## Results

Laticifers of *T. catharinensis* mature embryos and the shoot apex of 80-day-old plants exhibited distinct characteristics related to the subcellular organization and cell wall polysaccharide distribution; thus, the results are shown separately for the mature embryo and shoot apex considering the ultrastructure and immunolocalization of pectin epitopes and callose.

### Laticifer ultrastructure

#### Mature embryo

Laticifers were distinguished from ground meristematic cells by their axially elongated form (Fig. 1a, b), irregular outline, and projections where there was contact with two or more cells (Fig. 1b, c). Laticifers that were irregular in outline with tips with acuminate ends that were wedged between the middle lamella of adjacent meristematic cells were eventually observed (Fig. 1c), indicating intrusive growth. The laticifer walls had a loose structure (Fig. 1d), and enlarged plasmodesmata channels (Fig. 1d) or pores (Fig. 1e) connecting the laticifer to an adjacent cell were observed. The middle lamella could (Fig. 1d–f) or could not (Fig. 1g) be distinguished from adjacent primary walls.

The laticifer protoplasts had variable content and low organelle definition (Fig. 1). Laticifers may have reduced cytoplasm interspersed with abundant lipid and protein bodies, which had smaller dimensions when compared to the ground meristem cells (Fig. 1a). During laticifer development, there were signs of degradation of the reserve material (Fig. 1a–f), and electron-dense flocculated material dispersed in a finely granular medium filled the laticifer protoplasts (Fig. 1e, f). Signs of degradation of the reserve content in the protoplasts of adjacent meristematic cells were observed in the pore region (Fig. 1f), indicating the incorporation of meristematic cells into the laticifer system. A proliferation of electron-dense strands of rough endoplasmic reticulum (RER) and small vacuoles (Fig. 1b, g) was observed concurrently with the degradation of reserve material in the laticifers.

#### Plant shoot apex

Laticifers were distinguished from surrounding cells because they were axially elongated and irregular in outline and had electron-dense and thickened cell walls (Fig. 2a–c). The middle lamella was thickest in the cell corners, where laticifers were in contact with two or more cells (Fig. 2c). Occasionally, obstructed plasmodesmata were observed as unusual electron-dense fibrillar arrangements within the common walls between laticifers and adjacent cells (Fig. 2d), or peculiar electron-dense swellings within the adjacent wall (Fig. 2e). Electron-lucent materials were observed immersed in the laticifer walls (Fig. 2d). End and lateral discontinuous walls were observed between the laticifers (Fig. 2f).

The laticifers exhibited differences in protoplast density and organelle populations in the same section of the apex (Fig. 2a). Some laticifers had a strong electron-dense content, numerous spherical mitochondria, plastids lacking grana and with plastoglobuli, small vacuoles with either electron-dense granular content or membranous materials (cytoplasmic debris), and vacuole fusion (Fig. 2a, f). Sinuous plasma membranes (Fig. 2g, h) and periplasmic space containing membrane debris and electron-dense content were observed (Fig. 2g). Other laticifers had less dense content, with numerous vesicles and vacuoles containing electron-dense granular material (Fig. 2a, d); in the protoplast, spherical mitochondria (Fig. 2b), RER (Fig. 2h), Golgi bodies exhibiting dilated extremities and numerous adjacent vesicles (Fig. 2i), and polyribosomes (Fig. 2h, i) were observed. Vesicles derived from dilated regions of the RER (Fig. 2h) and numerous vesicles associated with Golgi bodies (Fig. 2i) were also observed. Vacuolated laticifers had electron-opaque inclusions surrounded by electron-dense content (latex particles) in the vacuoles (Fig. 2b), or, less commonly, dispersed in the cytoplasm.

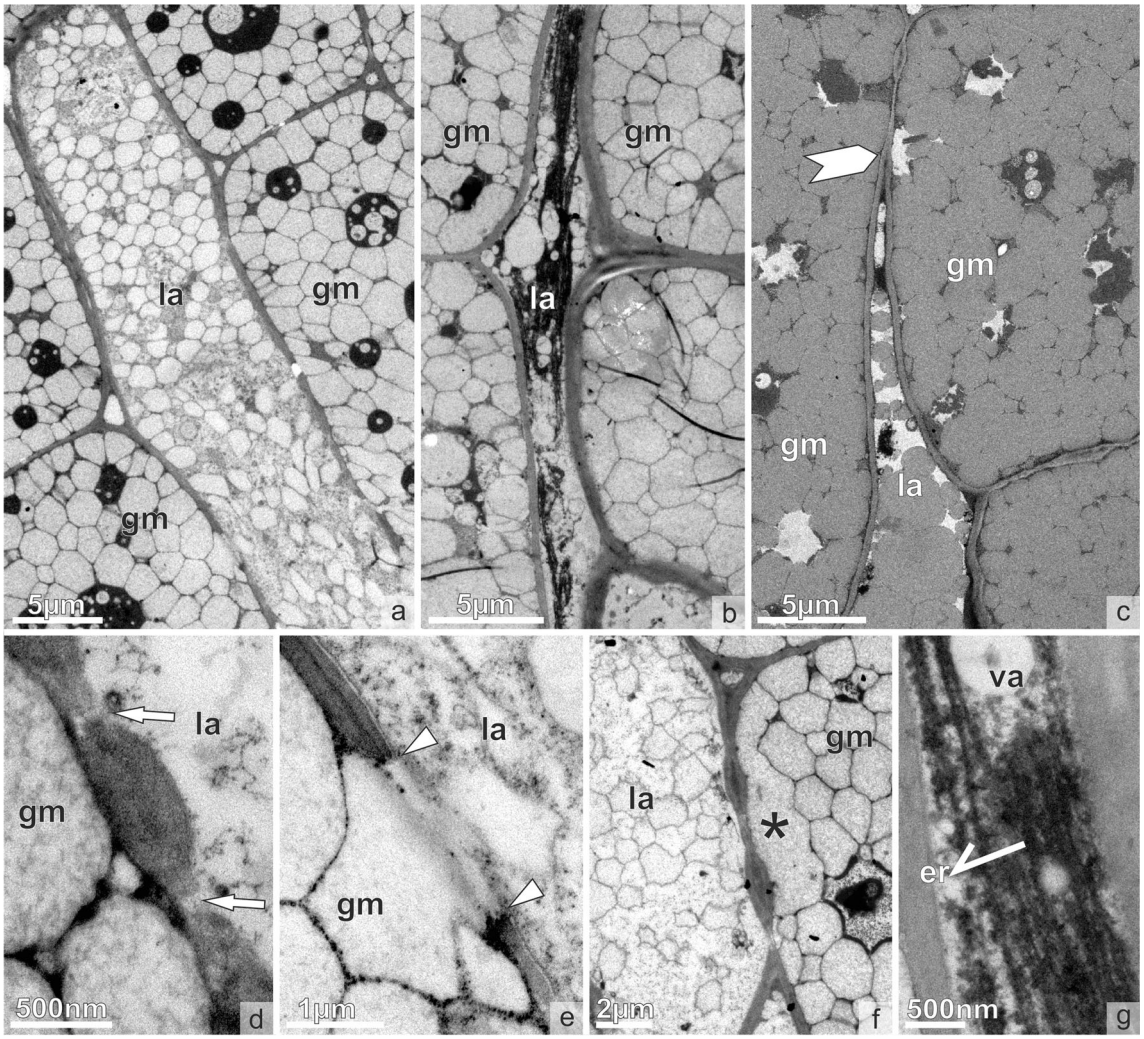


**Fig. 1** Ultrastructural characterization and features associated with the growth mechanisms of laticifers in the mature embryo of *Tabernaemontana catharinensis*. **a** Laticifer (la) with reduced cytoplasm interspersed with lipid and protein bodies. **b** Laticifer irregular in outline and with projections where there is contact with two or more cells. **c** Laticifers with a tip with acuminate ends (marker) that is wedged between the middle lamella of ground meristematic cells (gm). **d**, **e** Enlarged plasmodesmata channels (**d**; arrows) and pores (**e**; arrowheads) connecting the laticifer to an adjacent meristematic cell. **f** Ground meristem cell (gm) in contact with a laticifer and with signs of degradation of the reserve material (asterisk) near the pore region. **g** Laticifer protoplast containing electron-dense strands of endoplasmic reticulum (er) and small vacuoles (va). la = laticifer; gm = ground meristem cell

In the most proximal region of the shoot apex, where cells are differentiated (differentiated portion), laticifers with a large central vacuole and reduced peripheral cytoplasm with the abovementioned organelles were found (Fig. 2j). The vacuole contained membrane debris, flocculated material, and latex particles (Fig. 2j). The cell wall did not seem to be structurally different to parenchyma cell walls (Fig. 2j, k).

Images suggesting intrusive growth and the incorporation of adjacent cells into the laticifer system were frequently observed in the most distal region (undifferentiated portion) of the shoot apex (Fig. 3). Laticifer tips intruded into the middle lamella of adjacent meristematic cells, forming elongated, thin projections (Fig. 3a, b). The middle lamella in the growing region was thick and strongly electron-dense (Fig. 3a, b). Cortical microtubules (i.e., microtubules located in the peripheral cytoplasm just inside the plasma membrane) were observed in meristematic cells in contact with the laticifer projections (Fig. 3c). The microtubules were oriented more or less perpendicularly to the direction of elongation of the laticifer projection (Fig. 3c). During the incorporation of adjacent meristematic cells into the laticifer system, it was possible to identify meristematic cells with loose and disassembled walls (Fig. 3d) and cortical microtubules perpendicularly oriented to the wall at points of contact with the laticifers (Fig. 3e). The laticifers projected inwards into contiguous meristematic cells, which were intermediate between laticifers and meristematic cells (Fig. 3f). The walls in the projection region were loose and exhibited signs of degradation (Fig. 3f, inset).

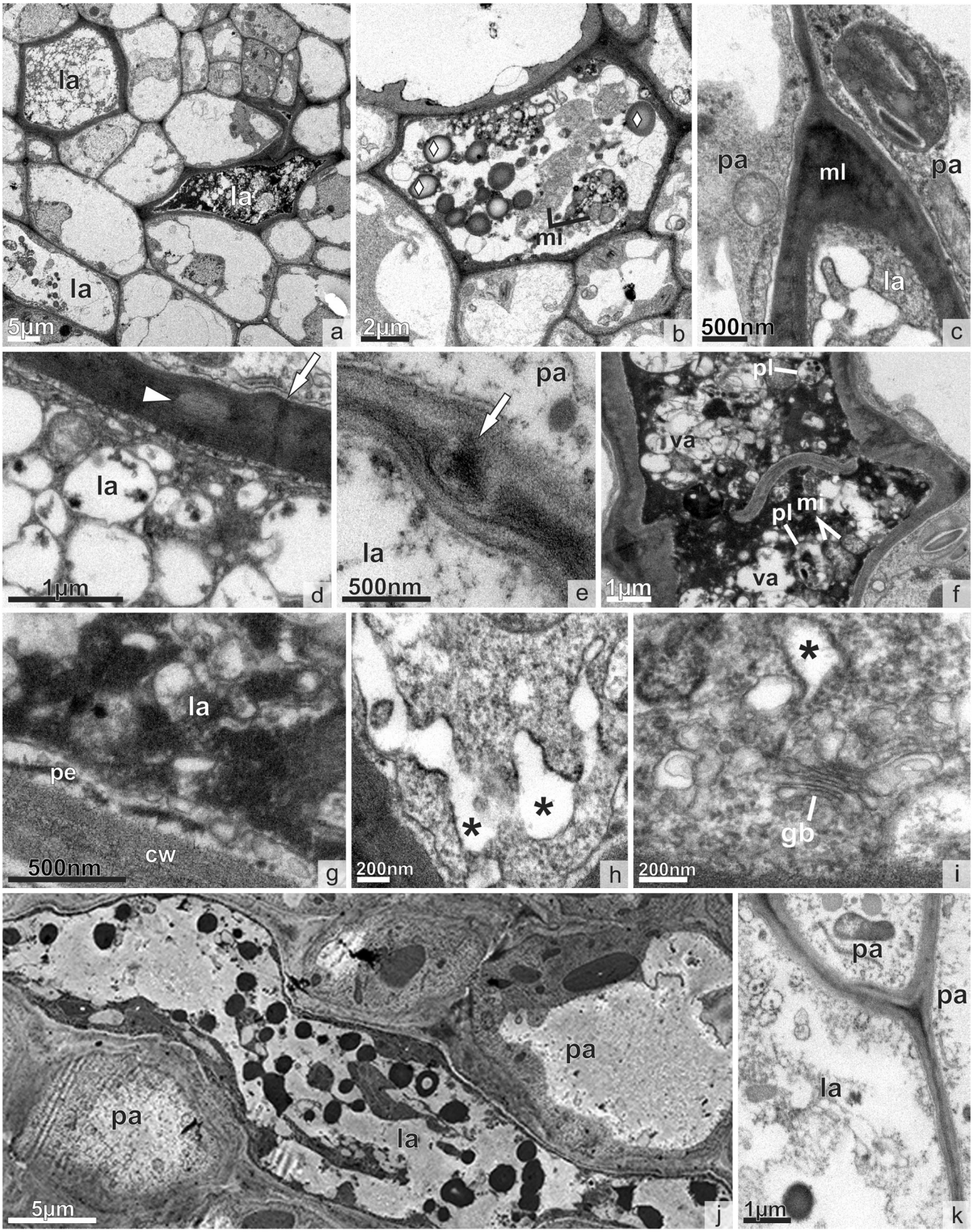
la
la
la
5µm
a
2µm
mi
b
pa
ml
pa
la
500nm
c
la
1µm
d
pa
la
500nm
e
pl
va
pl
mi
va
1µm
f
la
pe
cw
500nm
g
200nm
h
*
gb
200nm
i
pa
pa
la
5µm
j
pa
pa
la
1µm
k

◀ **Fig. 2** Ultrastructural characterization of laticifers in the plant shoot apex of *Tabernaemontana catharinensis*. **a** Laticifers (la) with distinct ultrastructural features. **b** Laticifer irregular in outline with electron-dense and thickened cell walls. Note the mitochondria (mi) and electron-opaque inclusions surrounded by electron-dense content (diamond) dispersed in the cytoplasm. **c** Thick laticifer wall and swollen middle lamella (ml) in the cell corners. **d** Electron-lucent materials (arrowheads) and unusual electron-dense fibrillar arrangements (arrow) within the common walls between laticifers and adjacent cells. Laticifer protoplast filled with numerous small vacuoles containing electron-dense granular material. **e** Peculiar electron-dense swellings (arrow) within the walls of the laticifer and adjacent cell. **f** Discontinuous cell walls between laticifers. Laticifer cytoplasm with mitochondria (mi), plastids (pl), and small vacuoles (va) with electron-dense granular content or membranous materials. **g** Periplasmic space (pe) in a laticifer containing membrane debris and electron-dense material. **h** Vesicles derived from dilated regions of the rough endoplasmic reticulum (asterisk). Note the sinuous plasma membrane. **i** Golgi body (gb) with associated vesicles. Note the dilated regions of the rough endoplasmic reticulum (asterisk) near the vesicles from the Golgi body and polyribosomes dispersed in the cytoplasm. **j**, **k** Laticifer in differentiated portion of the shoot apex. **j** Section nonstained with uranyl acetate and lead citrate. Laticifer with a large central vacuole and reduced peripheral cytoplasm. Note the membrane debris, flocculated material, and latex particles within the vacuole. **k** Similar wall structure in laticifer and parenchyma cells. cw = cell wall; la = laticifer; pa = parenchyma cell

## Immunolocalization of pectin epitopes and callose

### Mature embryo

Light microscopy revealed that laticifers were distinguishable from adjacent cells by their axially elongated form (Fig. 4a). JIM5 (HGs with a low degree of methyl esterification) exhibited weak labeling in all tissues but strong labeling at junction zones in corners between ground meristem cells and laticifers (Fig. 4b, Table 1). Immunogold for TEM revealed that the JIM5 epitope was most abundant in the middle lamella, particularly in cellular corners (Fig. 4c). The density of labeling was similar in the middle lamella of the laticifers (21 ± 5 gold particles $\mu m^{-2}$) and meristematic cells (21 ± 1 gold particles $\mu m^{-2}$).

LM5 and LM6, which recognize galactan and arabinan side chains, respectively, that are associated with rhamnogalacturonan I, exhibited distinct spatial labeling (Fig. 4d–f, Table 1). The LM5 epitope did not label the laticifer or ground meristem cell walls, even after pretreatment with pectate lyase (Fig. 4d). The LM6 epitope labeled the walls in a discontinuous pattern for different cell types, including laticifers (Fig. 4e), and sections without pectate lyase pretreatment did not exhibit labeling with LM6 (Fig. 4f), which seemed to be masked by pectic HGs. The labeling failures found in the laticifer walls (Fig. 4e) seemed to correspond to the region of plasmodesmata seen in the TEM analysis (Fig. 4g). Quantification of labeling with LM6 yielded 28 ± 8 gold particles $\mu m^{-2}$ in laticifer walls and 17 ± 2 gold particles $\mu m^{-2}$ in meristematic cell walls. Immunogold analysis by TEM showed no labeling with LM5 in the laticifer or meristematic cell walls in any of the treatments (data not shown).

BS400-2 (callose) produced a punctuated labeling pattern in the walls of laticifers and ground meristem cells adjacent and nonadjacent to the laticifers (Fig. 4h, i; Table 1). Samples prefixed with DDG (Fig. 4i) exhibited the same labeling pattern as BS400-2, the samples of which were not prefixed (Fig. 4h), indicating that no callose epitopes were deposited by injury as a result of collection or fixation. In the TEM analysis, BS400-2 labeled the region where plasmodesmata occurred (Fig. 4j–l), which would explain the punctuated pattern observed in the fluorescence. The number of the gold particles ranged from 4 to 11 in the plasmodesmata regions.

### Plant shoot apex

In longitudinal sections, light microscopy revealed that laticifers were distinguishable from surrounding cells by their elongated form and irregular outline (Fig. 5a–e). The JIM5 epitope exhibited a nonuniform labeling pattern in the undifferentiated and differentiated portions of the shoot apex (Fig. 5b). In the undifferentiated portion (Fig. 5c), the laticifer walls exhibited more intense labeling at the cellular corners than the adjacent meristematic cells (Fig. 5d) and the density of labeling was higher in the laticifers walls (36 ± 9 gold particles $\mu m^{-2}$) than in the meristematic cells (22 ± 9 gold particles $\mu m^{-2}$). In the differentiated portion (Fig. 5e), laticifers were similarly labeled to the adjacent cells with JIM5 (Fig. 5f). Quantification of labeling with JIM5 yielded 29 ± 5 gold particles $\mu m^{-2}$ in laticifer walls and 26 ± 5 gold particles $\mu m^{-2}$ in parenchyma cell walls. Using immunolocalization analysis by TEM, JIM5 labeling was particularly strong in the middle lamella (Fig. 5g), mainly in swollen regions at the cellular corners.

Light microscopy revealed that in undifferentiated portions of the apex, laticifers had a thicker primary cell wall than neighboring cells (Fig. 6a). LM5 (Fig. 6b, c) and LM6 (Fig. 6d, e) exhibited distinct spatial labeling (Table 1). LM5 weakly labeled galactan epitopes in the walls of meristematic cells (Fig. 6b, c), but laticifer walls exhibited no LM5 labeling (Fig. 6b, c). Immunogold electron microscopy confirmed the absence of this epitope in laticifer walls (Fig. 6f), and its presence in the inner cell wall layer near the plasma membrane of meristematic cells (Fig. 6f) with density of 28 ± 16 gold particles $\mu m^{-2}$. In contrast to LM5, LM6 labeled arabinan epitopes more strongly in laticifer walls than in meristematic cell walls (Fig. 6d, e). Immunogold analysis by TEM showed LM6 epitopes distributed throughout the cell walls of laticifers and adjacent meristematic cells (Fig. 6g), and common walls between meristematic cells exhibited less LM6 labeling (Fig. 6h), where quantified 91 ± 42 and 20 ± 10 gold particles $\mu m^{-2}$, respectively. Sections previously incubated with pectate lyase (Fig. 6c, e) exhibited a similar labeling

pattern to the sections that did not undergo this step and were incubated with LM5 (Fig. 6b) and LM6 (Fig. 6d). However, more intense fluorescence was detected with LM5 labeling in incubated sections (Fig. 6c) than in sections that were not incubated with pectate lyase (Fig. 6b).

Light microscopy revealed that in differentiated portions of the apex, wall thickness was similar between laticifers and neighboring cells (Fig. 6i). LM5 (Fig. 6j, l) and LM6 (Fig. 6k, m) exhibited distinct spatial labeling (Table 1). The laticifer walls exhibited moderate labeling and similar patterns and intensities as parenchyma cells for LM5 (Fig. 6j), which was distributed throughout the cell walls of laticifers and parenchyma cells (Fig. 6n, o) using TEM analysis. Density of labeling with LM5 was similar for laticifers ($20 \pm 1$ gold particles $\mu m^{-2}$) and parenchyma cells ($19 \pm 3$ gold particles $\mu m^{-2}$). The laticifer walls did not label as well as the parenchyma cell walls for LM6 (Fig. 6k), and virtually no gold particles were detected in walls of the laticifers or parenchyma cells after incubation with LM6 (data not shown). Sections previously incubated with pectate lyase (Fig. 6j, m) exhibited similar labeling patterns and intensities of reaction

**Fig. 4** Immunolocalization of pectin epitopes and callose in the walls of laticifers and adjacent cells in the mature embryo of *Tabernaemontana catharinensis*. **a**, **b**, **d**–**f**, **h**, **i** Longitudinal sections through the cotyledonary node. **a** Light microscopy. Section stained with toluidine blue. Note that the laticifers (arrows) were axially elongated. **b** Immunofluorescence microscopy. JIM5 weakly labeled the cell walls, including laticifers. **c** Immunogold labeling for TEM. JIM5 labeled (markers) the middle lamella between laticifers (la) and ground meristem cells (gm). **d**–**f** Immunofluorescence microscopy. **d** LM5 labeled after incubation with pectate lyase (PL). Note that there were no labeled laticifer (arrow) or ground meristematic cell walls, but there were labeled procambium (pc) cell walls. Section counterstained with Calcofluor White (Cal). **e**, **f** LM6 labeled in the walls of laticifers and adjacent cells. Section preincubated with pectate lyase (PL) labeled the walls in a discontinuous pattern (**e**), and in a section without this step did not exhibit labeling with LM6 (**f**). **g** Immunogold labeling for TEM. Section preincubated with pectate lyase (PL). LM6 labeled (markers) the laticifer walls in a discontinuous pattern, and no labelling occurred in the plasmodesmata region. **h**, **i** Immunofluorescence microscopy. BS400-2 labeled sections counterstained with Calcofluor White (Cal). Note the punctuated labeling pattern in the walls of laticifers and adjacent and nonadjacent meristematic cells in sections not prefixed with DDG (**h**) and prefixed with DDG (**i**). **j**–**l** Immunogold labeling for TEM. BS400-2 labeling (markers) the plasmodesmata region. **l** Section prefixed with DDG. la or arrow = laticifer; gm = ground meristem cell; marker = gold particle

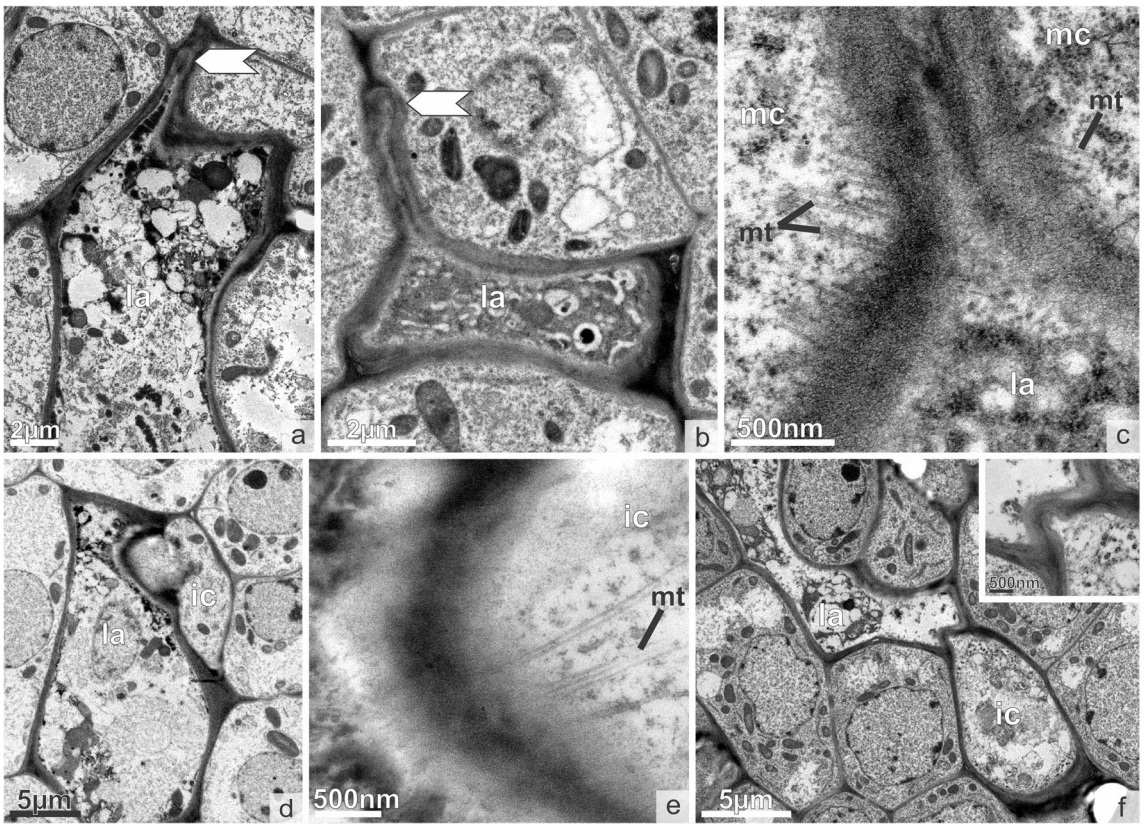


**Fig. 3** Ultrastructural features associated with the growth mechanisms of laticifers in undifferentiated portion of the plant shoot apex in *Tabernaemontana catharinensis*. **a**–**c** Elongated and thin projection of laticifer tips (markers) among the middle lamella of adjacent cells. **c** Cortical microtubules (mt) perpendicularly oriented in meristematic cells in contact with the laticifer projection. **d**–**f** Meristematic cells incorporated (ic) into the laticifer system. **d** Meristematic cell incorporated (ic) with loose and disassembled walls in regions of contact with the laticifer (la). **e** Cortical microtubules (mt) perpendicularly oriented to the wall in regions of contact with the laticifer. **f** Laticifer projecting into contiguous meristematic cells. Note the intermediate characteristics of laticifers and meristematic cells in the incorporated cell (ic), and the loose and disassembled cell wall in the region of the laticifer projection (inset). la = laticifer; mc = meristematic cell

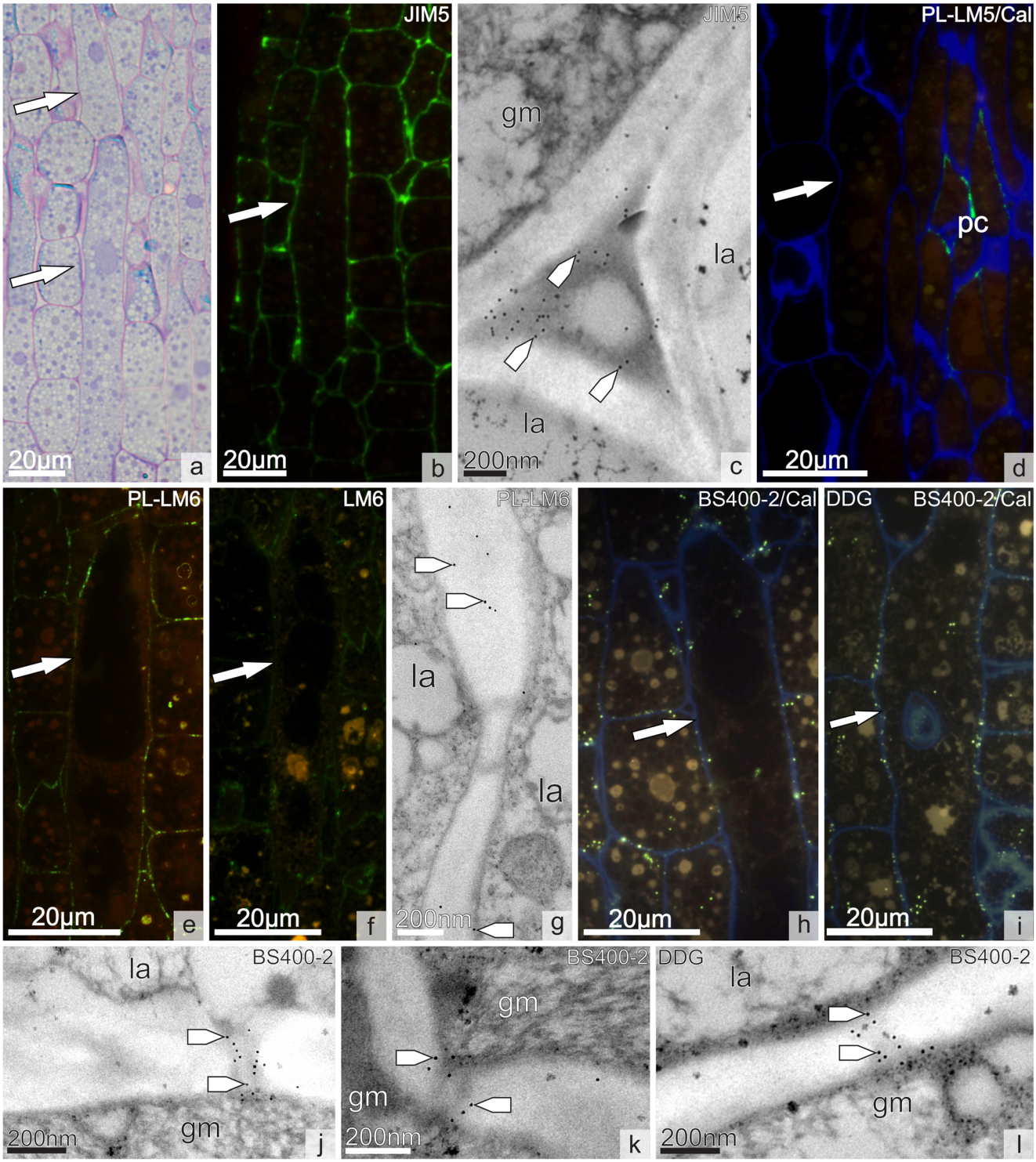


to the sections that did not undergo this step and were incubated with LM5 (Fig. 6l) and LM6 (Fig. 6k). In addition to different spatial arrangements, it was possible to identify a distinct temporal distribution between pectic galactan and arabinan labeled with LM5 and LM6, respectively.

Laticifers were immersed in different tissues, including the ground meristem (Fig. 7a) and were associated with phloem (Fig. 7c). BS400-2 exhibited a punctuated labeling pattern in most cell walls (Fig. 7b–e). The walls of laticifers and adjacent cells did not label for BS400-2, while the walls of nonadjacent cells exhibited labeling in closer regions of the apical meristem (Fig. 7b; Table 1). Little labeling was observed in laticifer and adjacent cell walls in differentiated tissue, and nonadjacent cells were labeled more intensely for BS400-2 (Fig. 7d,

e; Table 1). Samples prefixed with DDG (Fig. 7e) showed the same labeling pattern for BS400-2 as samples that were not prefixed (Fig. 7b, d), indicating that callose epitopes were not deposited by injury as a result of collection or fixation. Immunogold analysis by TEM did not reveal any labeling for BS400-2 in the common walls between laticifers and adjacent cells (Fig. 7f). Binding for this epitope was observed in regions with plasmodesmata in either parenchyma (Fig. 7g) or meristematic cell walls. In the plasmodesmata regions, the number of gold particles ranged from 5 to 11. Incubation with goat anti-mouse IgG (*whole molecule*)-Gold for analysis by TEM of BS-4002 (Fig. 7f, g) may have resulted in the large amount of particulate material observed in the sections.

## Discussion

In this study, we recorded for the first time cytological features and glycan epitope changes during the development of articulated anastomosing laticifers in *T. catharinensis* and compared the mature embryo and plant shoot apex, which exhibited diverse growth mechanisms, such as intrusive growth,

**Fig. 6** Immunolocalization of galactan (LM5) and arabinan (LM6) side chains associated with rhamnogalacturonan I in the walls of laticifers and adjacent cells in the plant shoot apex of *Tabernaemontana catharinensis*. **a**–**h** Undifferentiated portion of the shoot apex. **a**–**e** Longitudinal sections. **a** Light microscopy. Section stained with toluidine blue. Thick wall of laticifers and common walls between laticifers (arrowheads). **b**–**e** Immunofluorescence microscopy. **b** LM5 without preincubation with pectate lyase exhibiting weak labeling in ground meristematic cells. **c** LM5 labeling after incubation with pectate lyase (PL). Laticifer walls (arrowheads) not labeled. **d** LM6 more intensely labeled laticifer cell walls than meristematic cell walls. **e** LM6 labeled with preincubation with pectate lyase (PL). **f**–**h** Immunogold labeling for TEM. **f** LM5 labeled (markers) the inner cell wall layer near the plasma membrane of meristematic cells (mc) in contact with each other and laticifers (la). **g** LM6 epitopes (markers) distributed throughout the walls of laticifers (la) and adjacent meristematic cells (mc). **h** LM6 weakly labeled (markers) the walls of meristematic cells (mc). **i**–**o** Differentiated portion of the shoot apex. **i**–**k**, **n** Longitudinal sections. **l** Transverse section. **i** Light microscopy. Section stained with toluidine blue. **j** Similar labeling for LM5 (preincubated with pectate lyase, PL) in the walls of laticifers and parenchyma cells. **k** No labeling for LM6 in the walls of laticifers or parenchyma cells. **l** LM5 labeling without preincubation with pectate lyase. **m** Section preincubated with pectate lyase (PL). No labeling of the LM6 epitope in laticifer cell walls or parenchyma cell walls. **n**, **o** Immunogold labeling for TEM. **f**–**g** Similar labeling for LM5 (markers) in the walls of laticifers (la) and parenchyma cells (pa). la or arrow = laticifer; mc = meristematic cell; marker = gold particle; pa = parenchyma cell

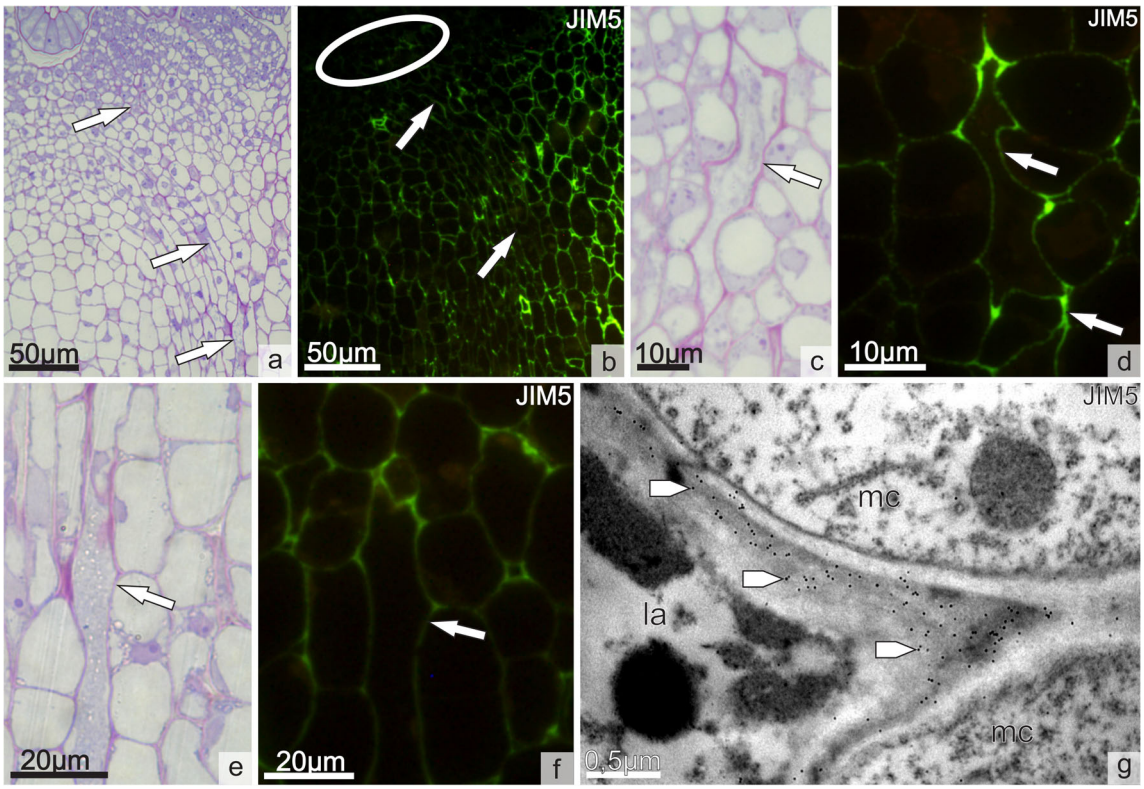


**Fig. 5** Immunolocalization of homogalacturonans with a low degree of methyl esterification (JIM5) in the walls of laticifers and adjacent cells in the plant shoot apex of *Tabernaemontana catharinensis*. **a**–**f** Longitudinal sections. **a**, **c**, **e** Light microscopy. Sections stained with toluidine blue. **a** Shoot apex showing laticifers (arrows) immersed in undifferentiated and differentiated tissues. **b**, **d**, **f** Immunofluorescence microscopy. **b** JIM5 weakly labeled the undifferentiated portion (circle) and moderately labeled the differentiated portions. **c**, **d** Laticifers (arrows) in the undifferentiated portion. **d** Laticifer walls were strongly labeled with JIM5 at cellular corner zones. **e**, **f** Laticifers (arrows) in the differentiated portion. **f** Laticifer labeled similarly to other cells with JIM5. **g** Immunogold labeling for TEM. JIM5 labeled (markers) the swollen middle lamella in cellular corners. la or arrow = laticifer; mc = meristematic cell; marker = gold particle

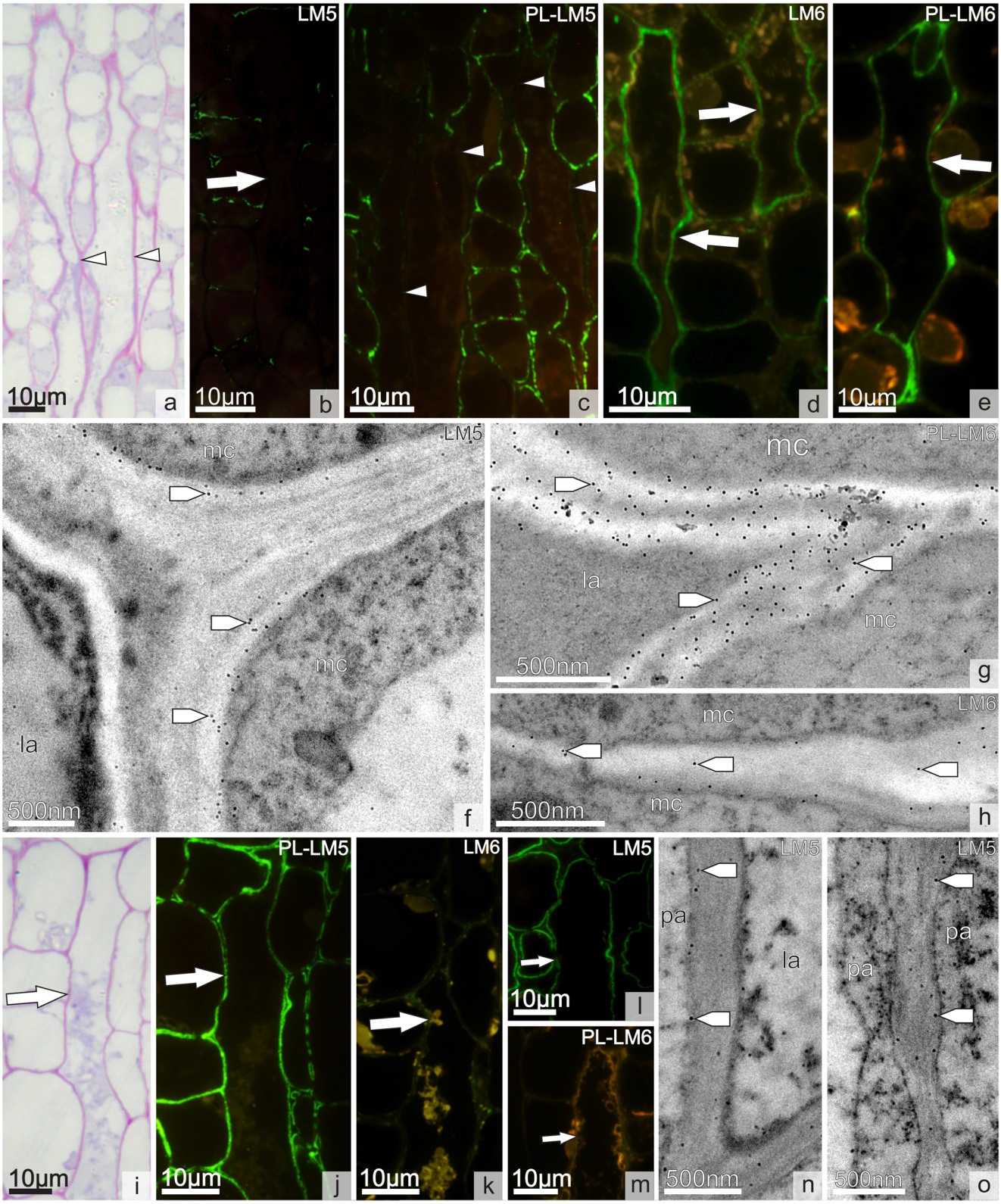


protoplast fusion, and the induction of adjacent cells to acquire laticifer features. Knowledge of cytological changes and cell wall polysaccharide distributions are essential to understand the growth mechanisms of the laticifer system.

Laticifers in the mature embryo and plant shoot apex differed in their protoplast arrangements and cell wall features in *T. catharinensis*. The degradation of reserve materials and proliferation of RER and vacuoles, as observed in laticifers

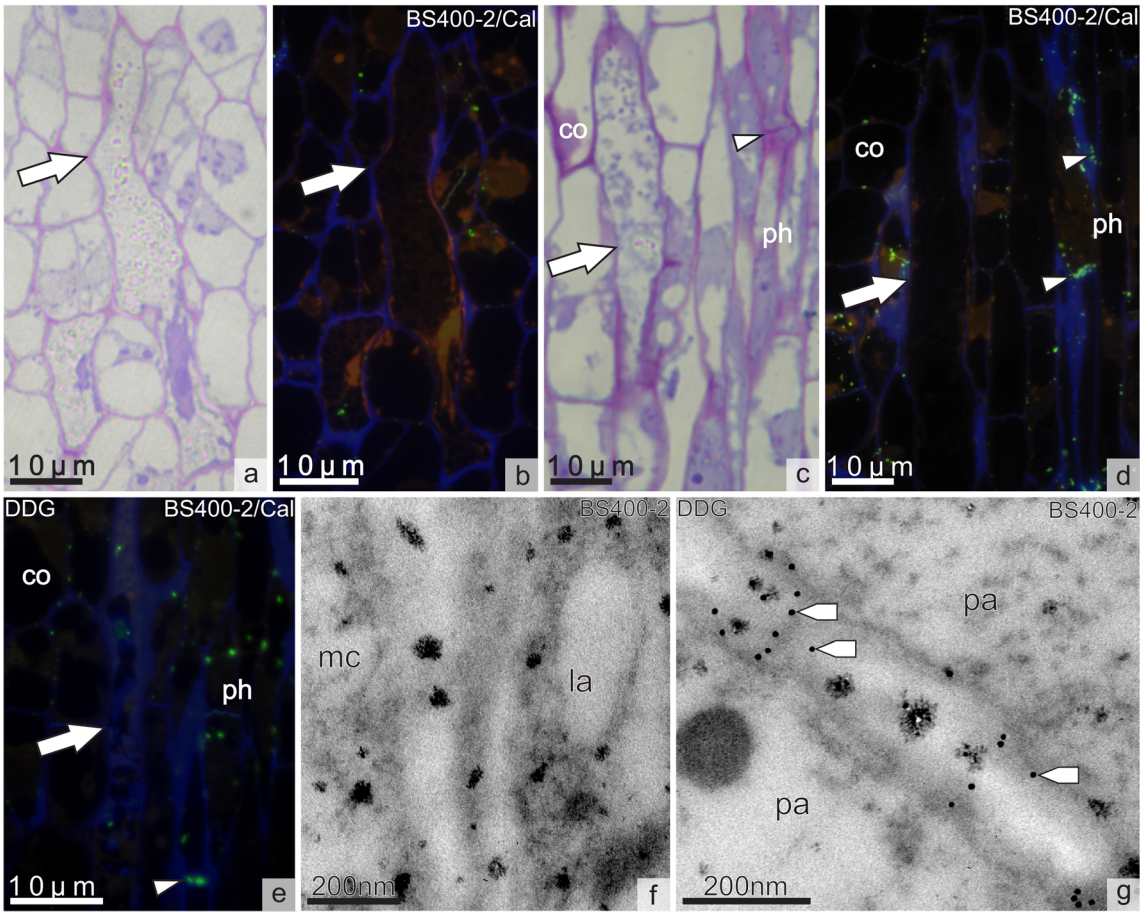


**Fig. 7** Immunolocalization of callose (BS400-2) in the walls of laticifers and adjacent cells in the plant shoot apex of *Tabernaemontana catharinensis*. **a**–**e** Longitudinal sections. **a**, **c** Light microscopy. Sections stained with toluidine blue. **b**, **d**, **e** Immunofluorescence microscopy. BS400-2 labeled sections counterstained with Calcofluor White (Cal). **a**, **b** Undifferentiated portion of the shoot apex. **c**–**e** Differentiated portion of the shoot apex. **b**, **d**, **e** Punctuated labeling pattern in meristematic and parenchyma cell walls and no labeling in laticifer (arrows) walls. **e** Section prefixed with DDG exhibited no change in the pattern of labeling for BS400-2. **f**, **g** Immunogold labeling for TEM. **f** No labeling in the common walls between laticifers (la) and meristematic cells (mc) for BS400-2. **g** Section prefixed with DDG. BS400-2 labeled (markers) plasmodesmata regions in parenchyma cell walls. la or arrow = laticifer; cm = meristem cell; pa = parenchyma cell; co = cortex region; ph = phloem; arrowhead = sieve plate; marker = gold particle

in *T. catharinensis* embryos, have also been reported in articulated laticifers in mature embryos of other Apocynaceae species (Milanez 1959, 1977). A well-developed central vacuole and peripheral cytoplasm, as observed in the differentiated laticifers of *T. catharinensis* plants, have frequently been reported in both articulated and nonarticulated laticifers in different taxa (Nessler and Mahlberg 1977; Milanez 1977; Wilson and Mahlberg 1978, 1980; Condon and Fineran 1989; Roy and Deepsh 1992; Nessler and Monacelli et al. 2005; Gama et al. 2017). The dilation of regions of the RER in *T. catharinensis* laticifers contributes to vacuole development, as reported for other latex-bearing plants (Nessler and Mahlberg 1977; Wilson and Mahlberg 1978, 1980; Cai et al. 2009). Moreover, vesicles derived from Golgi bodies also contribute to the increased vacuolation of these laticifers, as observed in other Apocynaceae species (Wilson and Mahlberg 1978; Gama et al. 2017). The proliferation of small vacuoles with cytoplasmic debris is evidence of autophagy (van Doorn and Papini 2013) in laticifers of the plant shoot apex in *T. catharinensis*, confirming a process that is commonly reported in laticifer development (Evert 2006; Gama et al. 2017). Numerous Golgi vesicles near the sinuous plasma membrane and the presence of materials inside the periplasmic spaces suggest the vesicle fused with this membrane, indicating that a granulocrine mechanism underlies the secretion of cell wall polysaccharides (Fahn 1979). In fact, pectins are synthesized in the Golgi apparatus, transported by vesicles to the plasma membrane, and inserted into the cell wall matrix (Ridley et al. 2001; Evert 2006; Mohnen 2008).

Our ultrastructural results clearly show that cell wall features, such as the thickness of the middle lamella and cell wall, loose and disassembled cell walls, the absence/presence of intercellular spaces, and symplastic connections, are directly linked to growth mechanisms in the laticifer system. These features are distinct in different developmental vegetative stages, and appear to be related to the growth mechanism that

is predominantly observed in laticifers in mature embryos and plant shoot apices of *T. catharinensis*.

The mechanism of meristematic cell incorporation into the laticifer system differed in *T. catharinensis* embryos and plants. In the embryo, this mechanism was characterized by the presence of pores (which arise from the enlargement of plasmodesmata) between common walls of laticifers and ground meristematic cells, and the degradation of reserve material from the meristematic cells starting in the pore region. Ground meristem cells have lipid and protein bodies as reserve material, while in laticifers, these substances are degraded at the beginning of laticifer differentiation in *T. catharinensis*. The occurrence of reserve materials in laticifers indicates the recent incorporation of a cell into the laticifer system (Milanez 1977). A similar laticifers' action-inducing mechanism has been described in articulated laticifers in mature embryos of *Cryptostegia grandiflora* (Milanez 1959) and *Nerium oleander* (Milanez 1977). Cell incorporation was the predominant growth mechanism of laticifers in mature embryos, in which the rates of cellular multiplication and elongation are low. In the *T. catharinensis* plant shoot apex, the mechanism that underlies the incorporation of meristematic cells into the laticifer system involved loose and disassembled cell walls, and the reorientation of cortical microtubules in the incorporated meristematic cells. In addition, the presence of cells that shared the same features of laticifers and meristematic cells that were connected by laticifer projections inwards towards meristematic cells is strong evidence of an inducting action of laticifers on other cells, as proposed by Milanez (1977). The occurrence of laticifers in different developmental stages (as revealed by ultrastructural differences between the laticifers) is indicative of the continuous addition of new cells to the laticifer system, in both mature embryos and plant shoot apices of *T. catharinensis*.

The occurrence of intrusive growth in articulated laticifers in *T. catharinensis* was supported by their irregular outline, thick middle lamella and cell walls in the cell corners, the absence of intercellular spaces, and the presence of thin laticifer projections intruding into the middle lamella of adjacent meristematic cells. These characteristics were more obvious in undifferentiated portions of the plant shoot apex than in the mature embryo and suggest that intrusive growth is associated with cell differentiation between these developmental vegetative stages. *Allamanda blanchetii*, another Apocynaceae species, has articulated anastomosing laticifers, but not intrusive growth (Gama et al. 2017). In the shoot apex of this species, the laticifer wall is initially thin and becomes irregular, with thickening in more differentiated regions of the laticifer (Gama et al. 2017); changes in the middle lamella were not reported. Such laticifer wall features in *A. blanchetii* differ to those observed in the present study in the undifferentiated portions of the *T. catharinensis* shoot apex, probably because of the absence of intrusive growth in the former species.

The occurrence of numerous plasmodesmata that connect laticifers and adjacent cells may make cell separation in the *T. catharinensis* embryo difficult, with less intrusive growth during this stage, whereas the absence of functional plasmodesmata and presence of obstructed plasmodesmata in plant laticifers may be favorable for intrusive growth. Symplastic connections are interrupted during laticifer intrusion between adjacent cells (Mahlberg 1993; Jarvis et al. 2003). However, broken plasmodesmata have also been reported in articulated laticifers in adult plants of *Calystegia silvatica* (Convolvulaceae) (Condon and Fineran 1989) and *Hevea brasiliensis* (Euphorbiaceae) (Faÿ et al. 1989), which do not exhibit intrusive growth. By this way, we conjecture that the decrease in symplastic connections between laticifers and adjacent cells in *T. catharinensis* may contribute to the isolation of toxic substances, which is consistent with the role assigned to laticifers in the isolation of defense chemicals of sensitive tissues (Farrell et al. 1991).

There were differences regarding the presence/abundance of pectin epitopes (labeled with JIM5, LM5, and LM6) and callose (labeled with BS400-2) between the cell walls of the laticifers and adjacent cells, between laticifer walls of the mature embryo and plant shoot apex, and between laticifer walls in proximal and distal regions of the apical meristem in the *T. catharinensis* shoot apex. Our immunocytochemical analysis revealed that the polysaccharide distribution in the walls of laticifers and adjacent cells may be related to the frequency of intrusive growth in the embryo and plant.

Low methyl-esterified HGs (recognized by JIM5) were detected most abundantly in the thick middle lamella and cell corners of the laticifers, particularly in undifferentiated portions of the *T. catharinensis* plant shoot apex. Although the occurrence of low methyl-esterified HGs in the middle lamella and reinforcing zones has been described in different cell types (Jarvis et al. 2003; Mohnen 2008), it is interesting that the same labeling pattern for JIM5 has been reported in laticifer walls in the shoot apex of *A. speciosa*, an Apocynaceae species with nonarticulated laticifers (Serpe et al. 2001, 2002). During intrusive growth, most of the laticifer remains connected to neighboring cells, while in tip-growth regions, the original cell-cell adhesion is dismantled and a new cell-cell bond must be established (Jarvis et al. 2003). It has been demonstrated that low-ester pectic polymers have a relatively high affinity for $Ca^{2+}$, and the middle lamella and reinforcing zones contain high levels of calcium (Jarvis et al. 2003). Furthermore, pectin $Ca^{2+}$ bridges seem to play a major role in cell adhesion (Jarvis et al. 2003; Levesque-Tremblay et al. 2015). Therefore, if low methyl-esterified HGs are linked to calcium in laticifer corners in *T. catharinensis*, these regions can act as anchor points and reestablish cell-cell bonding in the laticifers. The location of calcium and its co-location with low methyl-esterified HGs in cell walls should be further investigated in order to confirm or refute this hypothesis.

The absence of (1→4)-β-D-galactans (recognized by LM5) in laticifer walls in undifferentiated portions of the *T. catharinensis* shoot apex probably results in a less firm cell wall structure, ensuring the flexibility required for intrusive growth. Notably, even in a meristematic region such as the shoot apex, cells adjacent to the laticifers exhibited labeling for (1→4)-β-D-galactans with LM5; therefore, laticifers seem to maintain a feature of embryonic cells in this region, given that these epitopes did not label laticifers in the *T. catharinensis* embryo. Galactans have not been detected in the cell walls of meristematic regions (Willats et al. 1999), and their increased labeling is associated with firm tissues (McCartney et al. 2000; Orfila et al. 2001), improved cell adhesion (Bona et al. 2017), and decreased cell wall porosity (Sørensen et al. 2000). The absence of LM5 epitopes in laticifer walls has been reported in the plant shoot apices of *A. speciosa* (Serpe et al. 2002) and *E. heterophylla* (Euphorbiaceae) (Serpe et al. 2004). The low levels of (1→4)-β-D-galactans in laticifers would make their walls more porous, which may increase the extensibility of laticifer walls and facilitate the transfer of assimilates to the laticifers (Serpe et al. 2004). In *T. catharinensis*, the walls of meristematic and parenchyma cells in the shoot apex exhibited differing levels of galactan epitopes (recognized by LM5), with the most intense labeling observed in parenchyma cells. Galactans in the cell wall can make laticifer growth through parenchyma cells difficult, because parenchyma cell firmness and adhesion are increased.

The strong labeling of (1→5)-α-L-arabinans by LM6 in laticifer walls in undifferentiated portions of the *T. catharinensis* shoot apex indicates increased flexibility of the cell wall, as reported for other cell types (Jones et al. 2003, 2005; Verhertbruggen et al. 2009), and is a favorable feature for intrusive growth. Similar findings were reported for LM6 labeling in laticifer walls in the shoot apex of *A. speciosa* (Serpe et al. 2002). The flexibility caused by arabinan chains occurs because the chains maintain fluidity within the pectin network of the walls (Jones et al. 2003). Fluidity in the cell wall is an important feature, considering the absence of plasmodesmata in laticifers in the shoot apex, and facilitates apoplastic transport. The occurrence of arabinan epitopes (recognized by LM6) in meristematic cell walls and the nonlabeling of this epitope in parenchyma cell walls in the shoot apex also seem to be related to the frequency of intrusive growth in undifferentiated portions of the plant. Arabinans should maintain the wall flexibility of meristematic cells, because this reduces possible damage from laticifer growth through their walls. In addition, we suppose that arabinans are related to intrusive growth in laticifers, though their distributions may differ in different developmental stages. Laticifer and ground meristematic cell walls labeled weakly for LM6 in the mature embryo, whereas this epitope was abundant in the laticifer walls of the undifferentiated portion of the shoot apex in *T. catharinensis*. Nonarticulated laticifer walls in mature embryos of *Euphorbia lathyris* (Euphorbiaceae) (Castelblanque et al. 2016) specifically label for LM6; however, in the shoot apex of another species in this genus (*E. heterophylla*, Serpe et al. 2004), the walls of laticifers and adjacent cells are strongly labeled.

The punctuated labeling pattern for BS400-2, which recognizes callose, in the common walls of laticifers and ground meristem cells in the embryo, and its nonlabeling in laticifers in the shoot apex of *T. catharinensis*, suggest that callose labeling is associated with plasmodesmata. This finding is compatible with TEM analysis that showed numerous plasmodesmata in laticifers in the embryo (a feature that probably makes intrusive growth difficult), and their absence in laticifers in the plant shoot apex. In addition, the absence of callose accumulations in cell walls adjacent to laticifers in *T. catharinensis* when using BS400-2 suggests that intrusive growth does not damage neighboring cell walls, as reported for *A. speciosa* (Serpe et al. 2002) and *E. heterophylla* (Serpe et al. 2004).

Actively secreting laticifers occur in the mature embryo of *T. catharinensis* (Canaveze and Machado 2016); however, the same labeling patterns of wall glycans in surrounding meristematic cells suggest that laticifer walls in the mature embryo are still under development, as laticifer wall features change throughout plant development. Despite the fact that laticifer walls in the embryo shared the same characteristics of an absence of galactans and a presence of low methyl-esterified HGs and arabinans with laticifer walls in the plant shoot apex, which would confer the necessary flexibility and softness required for intrusive growth, the occurrence of numerous plasmodesmata and callose appears to be a limiting factor for intrusive growth.

The results of the present study and previous studies (Serpe et al. 2001, 2002, 2004; Castelblanque et al. 2016) suggest that the intrusive growth mechanism in articulated and nonarticulated laticifers involves similar modifications in cell wall features; however, some modifications may be taxon specific, or related to developmental stage. Therefore, studies should be conducted that include different developmental stages and a large number of species of a given taxa, in order to determine whether modifications in laticifer walls follow a phylogenetic or functional pattern.

In summary, the laticifers' cytology and polysaccharide distributions of laticifer walls differed between the mature embryo and plant shoot apex, which has implications for the growth mechanisms of *T. catharinensis*. When cell multiplication and elongation rates are low, as it is expected to occur in the mature embryo, cell incorporation into the laticifer system seems to be the predominant growth mechanism. Evidence for intrusive growth was stronger in undifferentiated portions of the plant shoot apex than in the mature embryo. The lower frequency of intrusive growth in the embryo seems to be

related to the occurrence of numerous plasmodesmata and callose in the cell walls. The glycan distribution in articulated laticifer walls indicates that the same intrusive process occurs as in nonarticulated laticifers, mainly in undifferentiated portions of the plant shoot apex. Intrusive growth appears to be associated to presence of arabinan (which increase wall flexibility and pectin network fluidity), and an absence of galactans (which reduces wall stiffness) and callose (as a consequence of a reduction in symplastic connections) in laticifer walls. The abundance of low de-methyl-esterified HGs in the middle lamella and corners may help reestablish cell-cell bonding in laticifers. Glycan distribution in the laticifer walls of the embryo indicated that the laticifers were still under development. TEM and immunocytochemical methods are complementary, and enabled us explore the cellular basis of the laticifers' action-inducing mechanism, and associate the distributions of glycan epitopes with intrusive growth.

**Acknowledgements** Thanks to the Electron Microscopy Centre (CME) IBB, UNESP, and its technicians for assistance with sample preparations. We are also thankful to Prof. J.-P Knox (University of Leeds, Centre of Plant Science, UK) for monoclonal antibodies against HG and RG-I kindly provided to the Laboratory of Plant Anatomy, UFRGS.

**Funding information** This study is financially supported by the National Council for Scientific and Technological Development (CNPq - financial support Proc. 473289/2010 and grants to the SR Machado Proc. 302657/2011-8) and the São Paulo Council for Research (FAPESP - financial support Thematic Project Proc. 2008/55434-7 and grants to the first author - Proc. 2012/16441-3).

## Compliance with ethical standards

**Conflict of interest** The authors declare that they have no conflict of interest.

## References

Bona C, Moço MCC, Mastroberti AA (2017) Cytological aspects during the stretching of collapsed cells in the root aerenchyma of *Potamogeton polygonus* Cham. & Schltdl. (Potamogetonaceae). Flora 239:151–158

Cai X, Li W, Yin L (2009) Ultrastructure and cytochemical localization of acid phosphatase of laticifers in *Euphorbia kansui* Liou. Protoplasma 238:3–10

Canaveze Y, Machado SR (2015) Leaf colleters in *Tabernaemontana catharinensis* (Apocynaceae, Rauvolfioideae): structure, ontogenesis, and cellular secretion. Botany 93:287–296

Canaveze Y, Machado SR (2016) The occurrence of intrusive growth associated with articulated laticifers in *Tabernaemontana catharinensis* A.DC., a new record for Apocynaceae. Int J Plant Sci 177:458–467

Castelblanque L, Balaguer B, Martí C, Rodríguez JJ, Orozco M, Vera P (2016) Novel insights into the organization of laticifer cells: a cell comprising a unified whole system. Plant Physiol 172:1032–1044

Condon JM, Fineran BA (1989) Distribution and organization of articulated laticifers in *Calystegia silvatica* (Convolvulaceae). Bot Gaz 150:289–302

Esau K (1965) Plant Anatomy. McGraw-Hill, New York

Evert RF (2006) Esau's plant anatomy. Wiley-Interscience, New York

Fahn A (1979) Secretory tissues in plants. Academic Press, London

Farrell BD, Dussourd DE, Mitter C (1991) Escalation of plant defense: do latex/resin canals spur plant diversification? Am Nat 138:881–900

Faÿ E, Sanier C, Hebant C (1989) The distribution of plasmodesmata in the phloem of *Hevea brasiliensis* in relation to laticifer loading. Protoplasma 149:155–162

Gale EF, Wayman F, Orlean PA (1984) The action of 2-Deoxy-D-glucose on the incorporation of glucose into (1→3)-β-D-glucan in stationary phase cultures of *Candida albicans*. J Gen Microbiol 130:3303–3311

Gama TSS, Rubiano VS, Demarco D (2017) Laticifer development and its growth mode in *Allamanda blanchetii* A.DC. (Apocynaceae). J Torrey Bot Soc 144(3):303–312

Harris N (1994) Immunocytochemistry for light and electron microscopy. In: Harris N, Oparka KJ (eds) Plant cell biology. A practical approach. Oxford University Press, London, pp 157–176

Hervé C, Rogowski A, Gilbert HJ, Knox JP (2009) Enzymatic treatments reveal differential capacities for xylan recognition and degradation in primary and secondary plant cell walls. Plant J 58:413–422

Hervé C, Marcus SE, Knox JP (2011) Monoclonal antibodies, carbohydrate-binding modules, and the detection of polysaccharides in plant cell walls. In: Popper ZA (ed) The plant cell wall—methods and protocols. Humana Press, New York, pp 103–114

Jarvis MC, Briggs SPH, Knox JP (2003) Intercellular adhesion and cell separation in plants. Plant Cell Environ 26:977–989

Jones L, Seymour GB, Knox JP (1997) Localization of pectic galactan in tomato cell walls using a monoclonal antibody specific to (1→4)-β-D-galactan. Plant Physiol 113:1405–1412

Jones L, Milne JL, McQueen-Mason S (2003) Cell wall arabinan is essential for guard cell function. Proc Natl Acad Sci U S A 100:11783–11788

Jones L, Milne JL, Ashford D, McCann MC, McQueen-Mason SJ (2005) A conserved functional role of pectic polymers in stomatal guard cells from a range of plant species. Planta 221:255–264

Levesque-Tremblay G, Pelloux J, Braybrook SA, Müller KM (2015) Tuning of pectin methylesterification: consequences for cell wall biomechanics and development. Planta 242:791–811

Lev-Yadun S (2001) Intrusive growth – the plant analog of dendrite and axon growth in animals. New Phytol 150:508–512

Lopes KLB, Thadeo M, Azevedo AA, Soares AA, Meira RMSA (2009) Articulated laticifers in the vegetative organs of *Mandevilla atroviolacea* (Apocynaceae, Apocynoideae). Can J Bot 87(2):202–209

Mahlberg PG (1993) Laticifers: an historical perspective. Bot Rev 59:1–23

Marcus SE, Verhertbruggen Y, Hervé C, Ordaz-Ortiz JJ, Farkas V, Pedersen HL, Willats WGT, Knox JP (2008) Pectic homogalacturonan masks abundant sets of xyloglucan epitopes in plant cell walls. BMC Plant Biol 8:1–12

McCartney L, Ormerod AP, Gidley MJ, Knox JP (2000) Temporal and spatial regulation of pectic (1→4)-β-D-galactan in cell walls of developing pea cotyledons: implications for mechanical properties. Plant J 22:105–113

McDowel EM, Trump BF (1976) Histologic fixatives suitable for diagnostic light and. electron microscopy 100:405–414

Meikle PJ, Bönig I, Hoogenraad NJ, Clarke AE, Stone BA (1991) The location of (1→3)-b-glucans in the walls of pollen tubes of *Nicotiana alata* using a (1→3)-b-glucan-specific monoclonal antibody. 185:1–8

Milanez FR (1959) Contribuição ao conhecimento anatômico de *Cryptostegia grandiflora* – I. Embrião. Rodriguésia 21/22(33–34):347–394

Milanez FR (1977) Ontogênese dos laticíferos contínuos de *Neridium* (*Nerium*) *oleander* L. Trabalhos do XXVI Congresso Nacional de Botânica, Rio de Janeiro 1975:343–379

Mohnen D (2008) Pectin structure and biosynthesis. Curr Opin Plant Biol 11:266–277

Monacelli B, Valleta A, Rascio N, Moro I, Pasqua G (2005) Laticifers in *Camptotheca acuminata* Decne: distribution and structure. Protoplasma 226:155–161

Nessler CL, Mahlberg PG (1977) Cell wall perforation in laticifers of *Papaver somniferum* L. Bot Gaz 138:402–408

O'Brien TP, Feder N, McCully ME (1964) Polychromatic staining of plant cell walls by toluidine blue O. Protoplasma 59:368–373

Orfila C, Seymour GB, Willats WGT, Huxham IM, Jarvis MC, Dover CJ, Thompson AJ, Knox P (2001) Altered middle lamella homogalacturonan and disrupted deposition of (1→5)-α-L-arabinans in the pericarp of *Cnr*, a ripening mutant of tomato. Plant Physiol 126:210–221

Radford JE, Vesk M, Overall RL (1998) Callose deposition at plasmodesmata. Protoplasma 201:30–37

Reynolds ES (1963) The use of lead citrate at high pH as an electron-opaque stain in electron microscopy. J Cell Biol 17(1):208–212

Ridley BL, O'Neill MA, Mohnen D (2001) Pectins: structure, biosynthesis, and oligogalacturonide-related signaling. Phytochemistry 57: 929–967

Roy AS, Deepsh N (1992) Studies on differentiation of laticifers through light and electron microscopy in *Calotropis gigantea* (Linn.) R.Br. Ann Bot-London 70:443–449

Schindelin J, Arganda-Carreras I, Frise E, Kaynig V, Longair M, Pietzsch T, Preibisch S, Rueden C, Saalfeld S, Schmid B, Tinevez JY, White DJ, Hartenstein V, Eliceiri K, Tomancak P, Cardona A (2012) Fiji: an open-source platform for biologicalimage analysis. Nat Meth 9: 676–682

Serpe MD, Muir AJ, Keidel AM (2001) Localization of cell wall polysaccharides in nonarticulated laticifers of Asclepias speciosa Torr. Protoplasma 216:215–226

Serpe MD, Muir AJ, Driouich A (2002) Immunolocalization of β-D-glucans, pectins, and arabinogalactan-proteins during intrusive growth and elongation of nonarticulated laticifers in *Asclepias speciosa* Torr. Planta 215:357–370

Serpe MD, Muir AJ, Andème-Onzighi C, Driouich A (2004) Differential distribution of callose and a (1→4)β-D-galactan epitope in the laticiferous plant *Euphorbia heterophylla* L. Int J Plant Sci 165: 571–585

Sørensen SO, Pauly M, Bush M, Skjøt M, McCann M, Borkhardt B, Ulvskov P (2000) Pectin engineering: modification of potato pectin by *in vivo* expression of an endo-1,4-β-D-galactanase. P Natl Acad Sci USA 97:7639–7644

van Doorn WG, Papini A (2013) Ultrastructure of autophagy in plant cells: a review. 9(12):1922–1936

Verhertbruggen Y, Marcus SE, Haeger A, Ordaz-Ortiz JJ, Knox J (2009) An extended set of monoclonal antibodies to pectic homogalacturonan. Carbohydr Res 344:1858–1862

Willats WGT, Marcus SE, Knox JP (1998) Generation of a monoclonal antibody specific to (1-5)-a-L-arabinan. Carbohydr Res 308:149–152

Willats WGT, Steele-King CG, Marcus SE, Knox JP (1999) Side chains of pectic polysaccharides are regulated in relation to cell proliferation and cell differentiation. Plant J 20:619–628

Willats WGT, Limberg G, Buchholt HC, Van Alebeek GJ, Benen J, Christensen TMIE, Visser J, Voragen A, Mikkelsen JD, Knox JP (2000) Analysis of pectic epitopes recognised by hybridoma and phage display monoclonal antibodies using defined oligosaccharides, polysaccharides, and enzymatic degradation. Carbohydr Res 327:309–320

Wilson KJ, Mahlberg PG (1978) Ultrastructure of non-articulated laticifers in mature embryos and seedlings of *Asclepias syriaca* L. (Asclepiadaceae). Am J Bot 65:98–109

Wilson KJ, Mahlberg PG (1980) Ultrastructure of developing and mature nonarticulated laticifers in the milkweed *Asclepias syriaca* L. (Asclepiadaceae). Am J Bot 67:1160–1170